Appl. Phys. B 71, 123–127 (2000) / Digital Object Identifier (DOI) 10.1007/s003400000358

**Applied Physics B**
Lasers
and Optics

*Rapid communication*

# Spatial subharmonics in a photorefractive semiconductor

**K. Shcherbin**

Institute of Physics, Prospekt Nauki 46, 03650 Kiev, Ukraine
(Fax: +380-44/265-2359, E-mail: kshcherb@iop.kiev.ua)

Received: 5 April 2000/Published online: 7 June 2000 – © Springer-Verlag 2000

**Abstract.** The generation of spatial subharmonics is reported in a photorefractive semiconductor (CdTe:Ge) for the first time to our knowledge. Space charge waves with a narrow spatial spectrum are detected in homogeneously illuminated ac-biased CdTe:Ge sample by observation of a well developed low divergent self-diffracted beam. The mobility-lifetime product of the free carriers and the effective trap concentration are estimated from the threshold ac-field measured for different subharmonics at different grating vectors of the generated grating.

**PACS:** 42.65.Hw; 42.70.Nq; 52.35.Mw; 72.80.Ey

Subharmonics generation has been found experimentally in a photorefractive $Bi_{12}SiO_{20}$ crystal [1] when two plane waves with a small frequency detuning intersect inside the sample in the presence of a dc electric field with an appropriate amplitude. The spontaneous beams propagate in the directions corresponding to the diffraction from the gratings with the grating vectors $\boldsymbol{K}_{\mathrm{N}} = \boldsymbol{K}/\mathrm{N}$, $\boldsymbol{K}$ being the grating vector of the principal grating recorded by the two incident light beams, with integer N. That is why the phenomenon was called spatial subharmonic generation. The subharmonics were observed further in $Bi_{12}TiO_{20}$ [2] and $Bi_{12}GeO_{20}$ [3] using the same moving-grating technique with a dc electric field. It was shown also that subharmonics may be generated with an ac electric field applied to the sample illuminated by a stationary interference pattern [4].

The goal of the present paper is to show that subharmonics generation is inherent not only to sillenite-type crystals, but that the phenomenon is general for photorefractive materials of different classes. The first experimental observation of spatial subharmonics in a photorefractive semiconductor is reported for an ac-biased germanium-doped cadmium telluride. The range where subharmonics exist is studied by changing the spatial frequency $K$ of the principal grating and/or the amplitude of the ac-field. It is known that subharmonics generation may result from the excitation and parametric instability of space charge waves (SCW) [5–7]. The self excitation of the SCW is detected in a homogeneously illuminated ac-biased CdTe:Ge sample via observation of a strong beam diffracted from these waves.

This paper has a following structure. At first the experimental set-up is presented in Sect. 1. Then the experiments are described, demonstrating the spatial subharmonics generation and self-excitation of the SCW. The range of subharmonics existence is studied and the threshold amplitudes of the ac field are measured for different subharmonic gratings at different spatial frequencies of the primary grating. In Sect. 2 the experimental results are compared with the theoretical model and good agreement is stated. The crystal parameters are estimated from the dependences of the threshold ac field amplitude on spatial frequency of the principal grating. Plausible reasons why subharmonics generation has not been revealed earlier in semiconductors are discussed.

## 1 Experiment

A CdTe:Ge sample N90 (notation of the producer) is cut from the ingot grown by the Bridgman technique in Chernovtsy State University, Ukraine. It is a rectangular in shape with the dimensions $4\,\mathrm{mm} \times 5\,\mathrm{mm} \times 10\,\mathrm{mm}$ along the $[11\bar{2}]$, [111], and $[1\bar{1}0]$ directions, respectively. The input and output faces parallel to the $(1\bar{1}0)$ crystallographic plane are optically finished while the side faces parallel to the (111) plane are painted with silver paste. These electrodes are connected to an electric field generator that ensures a square-shaped ac field in the sample up to $8\,\mathrm{kV/cm}$. The slew rate of the generator is greater than $200\,\mathrm{V/\mu s}$, so that a rather good square waveform can be obtained up to frequencies of a few kHz.

A schematic sketch of the optical waves intersection for subharmonics excitation in the sample is shown in Fig. 1. The output beam of a single-mode single-frequency diode-pumped $Nd^{3+}$:YAG laser emitting at $1.064\,\mu\mathrm{m}$ is expanded and split into two recording beams with the wave vectors $\boldsymbol{k}_1$ and $\boldsymbol{k}_2$. These beams polarised in the plane of incidence impinge upon the sample at an angle $2\theta$. In such a manner the grating vector $\boldsymbol{K} = \boldsymbol{k}_1 - \boldsymbol{k}_2$ and the light polarisation vector are kept nearly parallel to the [111] direction that optimises the co-directional beam coupling in cubic crystals [8] and in

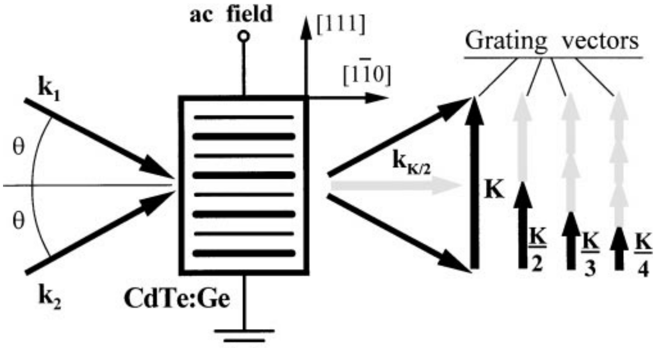


**Fig. 1.** Schematic representation of the wave intersection in the crystal. $\boldsymbol{k}_1$, $\boldsymbol{k}_2$ are the wave vectors of the recording beams, $\boldsymbol{k}_{\boldsymbol{K}/2}$ is the wave vector of the $\boldsymbol{K}/2$ subharmonic beam

CdTe in particular [9]. The intensities of the recording beams $I_1$ and $I_2$ are 12.8 mW/cm$^2$ and 5.5 mW/cm$^2$, respectively, with less than 10% intensity variation over the whole sample cross section.

The screen is placed behind the crystal at a distance of 1 m. The intensity distribution on the screen is close to the far-field distribution even with no lenses between the sample and the screen; it is recorded by a CCD camera.

Only one of the two recording beams is used in additional experiments with SCW excitation. The SCW are detected by the appearance of the diffracted spots in the far-field.

In the first experiment the principal grating with the grating spacing $\Lambda = 2\pi/K \approx 21\,\mu$m (spatial frequency $K \approx 300\,\text{mm}^{-1}$, free space angle $2\theta \approx 2.8°$) is recorded. The ac field frequency is set to 700 Hz. For the field amplitude $E_0$ exceeding 2.2 kV/cm the diffuse spot corresponding to the $\boldsymbol{K}/2$ subharmonic becomes visible on the screen. The far-field patterns for different amplitudes of the square-wave field are shown in Fig. 2. With the ac field increasing the $\boldsymbol{K}/2$ subharmonic beam becomes stronger and sharper until a new beam corresponding to the $\boldsymbol{K}/3$ grating appears at $E_0 > 3.2$ kV/cm. The maximum intensity of the $\boldsymbol{K}/2$ beam reaches 10% of the total intensity. It should be mentioned that $\boldsymbol{K}/2$ subharmonic does not disappear immediately when the $\boldsymbol{K}/3$ grating arises. These two gratings coexist simultaneously in a certain range of the applied voltage. However the intensity of the $\boldsymbol{K}/3$ spot increases with the electric field while the $\boldsymbol{K}/2$ spot blurs and its intensity decreases until this spot vanishes. Finally the light beam corresponding to the grating vector $\boldsymbol{K}/4$ appears at $E_0 \approx 5.2$ kV/cm and becomes stronger when the ac field increases. The $\boldsymbol{K}/3$ and $\boldsymbol{K}/4$ beams coexist within a certain voltage range in a similar way as it was described for the $\boldsymbol{K}/2$ and $\boldsymbol{K}/3$ beams.

The threshold ac field amplitudes necessary for the excitation of different subharmonic gratings are measured as a function of grating spacing of the principal grating $\Lambda$ to find the region where the light-induced grating is unstable against subharmonics. The obtained dependences are shown in Fig. 3 by squares, triangles, and diamonds for the $\boldsymbol{K}/2$, $\boldsymbol{K}/3$, and $\boldsymbol{K}/4$ gratings, respectively. The area of subharmonics existence covers a wide region of the grating spacings from $\Lambda \approx 4.5\,\mu$m ($K \approx 1400\,\text{mm}^{-1}$) to $\Lambda \approx 45\,\mu$m ($K \approx 140\,\text{mm}^{-1}$).

The subharmonics considered in the present paper result from the parametric excitation of the SCW [5–7]. According to the theory weakly damped SCW may be generated in

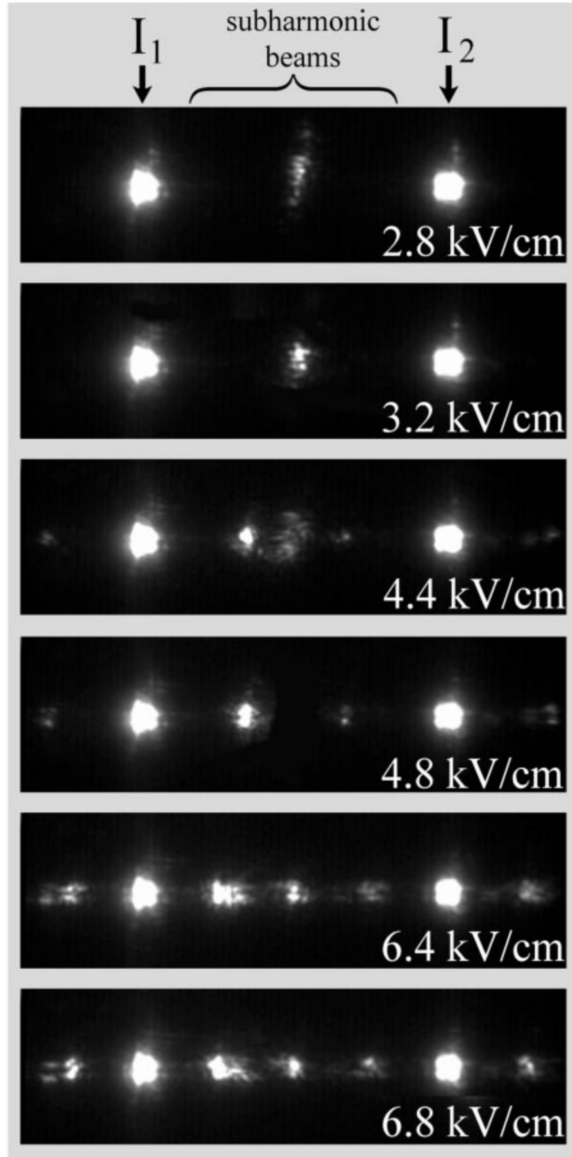


**Fig. 2.** Intensity distribution of the recording ($I_1$ and $I_2$) and subharmonic beams observed at different amplitudes of the ac field. The free space angle between the recording beams is $2\theta \approx 2.8°$ (grating spacing $\Lambda \approx 21\,\mu$m)

a photorefractive crystal with a large mobility-lifetime product $\mu\tau$ in the presence of an electric field [6, 10] without any primary grating. A spontaneous beam with a relatively small divergence that is self-developing because of the diffraction from the SCW has been reported for $Bi_{12}SiO_{20}$ [11, 12]. To check the possibility of SCW self-excitation in CdTe:Ge the following experiment is performed. The ac-biased sample is illuminated by only one beam $I_1$ with the intensity kept 12.8 mW/cm$^2$. The presence of the spontaneous self-diffracted beams is checked at different amplitudes of the applied voltage. The diffraction patterns recorded by the CCD camera are shown in Fig. 4. The diffuse spot that consists of relatively large speckles becomes visible starting from the field 3 kV/cm. Note that the tone balance has been adjusted in the two upper pictures of Fig. 4 to visualise the weak diffracted spot. Because of the photorefractive self-amplification the diffracted beam first appears from the side

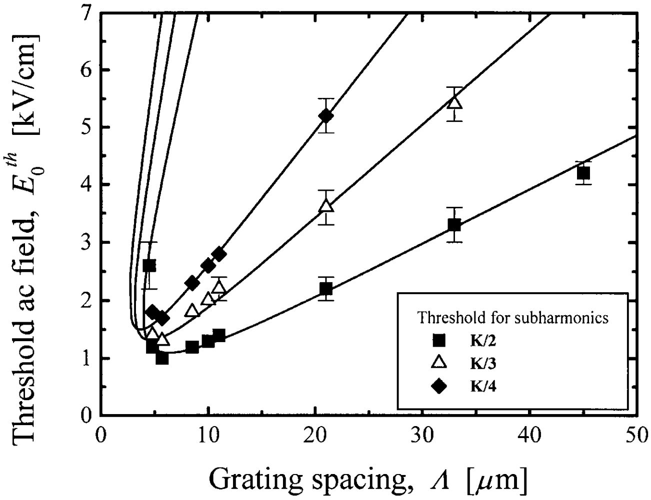


**Fig. 3.** Threshold values of the ac field amplitude $E_0^{\text{th}}$ for different subharmonic gratings as a function of the fringe spacing $\Lambda$ of the light-induced grating measured experimentally (*dots*) and calculated (*lines*) with $\mu\tau = 10^{-10}\,\text{m}^2/\text{V}$, $N_\text{E} = 4\times10^{20}\,\text{m}^{-3}$, and $Q = 2.7, 3$, and $3.2$ for the $\boldsymbol{K}/2$, $\boldsymbol{K}/3$, and $\boldsymbol{K}/4$ subharmonics, respectively

of the transmitted beam defined by the direction of the energy coupling. With the increasing ac field the self-excited beam becomes stronger and more confined and the angle between the transmitted and diffracted beams decreases. At $E_0 = 8\,\text{kV/cm}$ a well defined small divergent beam with an intensity about 10% of the input light intensity propagates at an angle of about 0.64° to the transmitted beam, thus confirming the presence of a clearly distinct SCW with a wavelength $\Lambda_\text{SCW}$ around 95 μm (spatial frequency $K_\text{SCW} \approx 66\,\text{mm}^{-1}$). The symmetrically diffracted beam is also observed at high voltages, as well as the high order diffracted beams.

In the first study of subharmonics generation with ac field [4] the different subharmonics were generated in a $Bi_{12}SiO_{20}$ crystal at different frequencies of the applied field. Such a pronounced switching behaviour is not observed in the studied CdTe sample. At the specified intensity of the recording light the subharmonic beams appear if the frequency of the ac field exceeds 80 Hz. Then the intensity of the generated beams becomes stronger with the frequency increasing until saturation is reached at about 500 Hz. At frequencies higher than 1000 Hz the amplitude of the subharmonic grating diminishes slowly since the square waveform of the electric field becomes imperfect because of the bandwidth limitation of the power supply. This is why the ac field frequency of 700 Hz is chosen in all experiments.

It has been reported earlier [13] that the subharmonic regimes may be controlled by changing the contrast $m$ of the interference pattern. Subharmonics switching is not achieved in the present experiments when the contrast is changed within $m = 0.5\ldots1$. However, the variation in intensity modulation could result in another kind of switching. The intensity of the subharmonic beams becomes smaller with the fringe visibility reduction until they disappear completely at a certain contrast, while the self-diffracted beam occurs if the ac field amplitude is large enough for effective SCW self-excitation.

To summarise, the subharmonics are excited in the studied CdTe:Ge sample at certain threshold ac field amplitudes. This threshold field depends on the spatial frequency of the recording grating; it is different for different secondary gratings. Self-excitation of the SCW may also affect subharmonics generation.

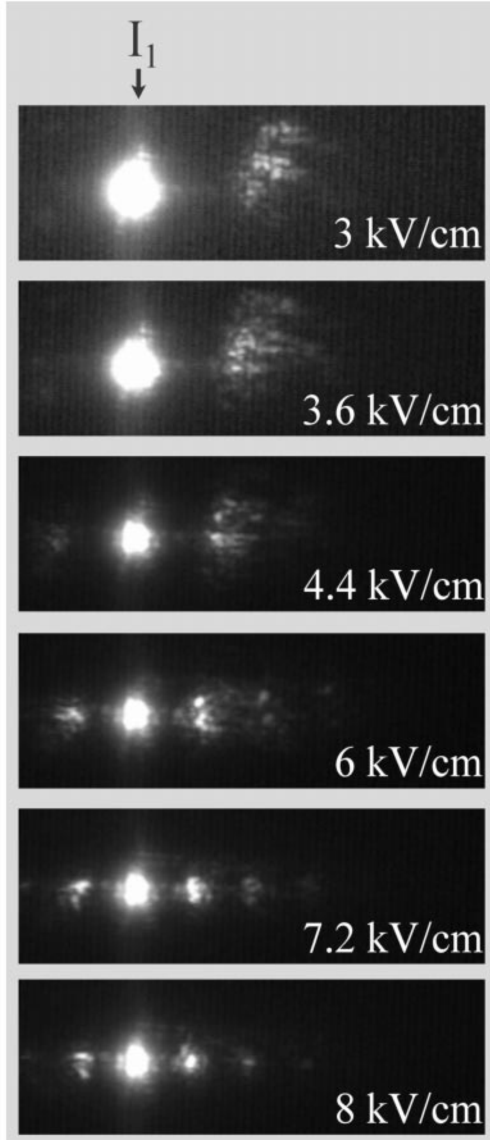


**Fig. 4.** Intensity distribution of the transmitted ($I_1$) and self-excited beam observed at different amplitudes of the ac field

## 2 Discussion

Two origins of subharmonic self-excitation are known at present. The first is related to optical parametric wave mixing [14], while the second one is concerned with parametric excitation of the SCW with $\boldsymbol{K}/2$, $\boldsymbol{K}/3$, etc., steming from the nonlinearity of the material equations [5, 7]. We believe that the subharmonics considered in the present paper result from SCW excitation [6].

The excitation of SCW occurs at any amplitude of the external field (see, for example, [15]) while subharmonic generation is a threshold phenomenon. We recall below how the theory [6] defines the threshold of subharmonic oscillation, fit the experimental data to the calculated threshold dependences and extract from this the SCW characteristics and material parameters (mobility-lifetime product and effective trap density).

An important parameter characterising SCW is the quality factor $Q$ which is introduced as the ratio of the eigenfrequency and the dumping constant of SCW [6]. It determines how far the eigenwaves propagate without a driving force. The quality factor depends on the crystal characteristics, the electric field amplitude $E_0$, and the SCW spatial frequency $K_{\mathrm{SCW}}$, which should be close to the spatial frequency of the subharmonic grating $K_{\mathrm{N}}$:

$$Q = \left( \frac{E_0}{E_{\mathrm{q}}} + \frac{E_{\mathrm{M}}}{E_0} + \frac{E_{\mathrm{D}}}{E_{\mathrm{M}}} \right)^{-1}, \tag{1}$$

where $E_{\mathrm{q}}$, $E_{\mathrm{D}}$, and $E_{\mathrm{M}}$ are the characteristic fields:

$$E_{\mathrm{q}} = \frac{eN_{\mathrm{E}}}{\varepsilon\varepsilon_0 K_{\mathrm{N}}}, \quad E_{\mathrm{D}} = K_{\mathrm{N}} \frac{k_{\mathrm{B}}T}{e}, \quad E_{\mathrm{M}} = \frac{1}{K_{\mathrm{N}}\mu\tau}, \tag{2}$$

$e$ is the electron charge, $N_{\mathrm{E}}$ is the effective trap density, $\varepsilon$ and $\varepsilon_0$ are the dielectric constants of the material and vacuum, respectively, $k_{\mathrm{B}}$ is the Bolzmann constant, and $T$ is the absolute temperature. The larger the $Q$ the stronger are SCW. For any particular spatial frequency of the primary grating $K = NK_{\mathrm{N}}$ there exists a certain threshold value $E_0^{\mathrm{th}}$ for which $Q$ reaches its threshold value $Q_{\mathrm{th}}$:

$$E_0^{\mathrm{th}} = \frac{1}{2Q_{\mathrm{th}}} \left( E_{\mathrm{q}} \pm \sqrt{E_{\mathrm{q}}^2 - 4Q_{\mathrm{th}}^2 E_{\mathrm{q}} (E_{\mathrm{D}} + E_{\mathrm{M}})} \right), \tag{3}$$

For large $\Lambda$, where $E_{\mathrm{q}} \gg E_{\mathrm{D}}, E_{\mathrm{M}}$ and $E_{\mathrm{M}} > E_{\mathrm{D}}$, the threshold field depends linearly on the grating spacing:

$$E_0^{\mathrm{th}} \approx Q_{\mathrm{th}} E_{\mathrm{M}} = \frac{Q_{\mathrm{th}} N}{2\pi\mu\tau} \Lambda . \tag{4}$$

The linearity of the experimental dependences of Fig. 3 at large grating spacing confirms the validity of the approximation given by (4). From the slope of the threshold dependences a factor $\mu\tau/Q = (3.3 \pm 0.6) \times 10^{-11}\,\mathrm{m^2/V}$ can be evaluated. The assumption that the threshold quality factor in the present experiments is close to that estimated in [6] for $Bi_{12}SiO_{20}$ $Q_{\mathrm{th}} \approx 3$ gives quite a reasonable value for the mobility-lifetime product of the studied CdTe sample $\mu\tau \approx 10^{-10}\,\mathrm{m^2/V}$.

The relation connecting $\mu\tau$, $N_{\mathrm{E}}$, and $Q_{\mathrm{th}}$ may be obtained also from the smallest grating spacing $\Lambda_{\min}$ at which the subharmonics are observed. $\Lambda_{\min}$ is the smallest spacing for which $E_0^{\mathrm{th}}$ given by (3) is the real value. Taking the expression under the square root in (3) equal to zero it is possible to estimate the effective trap density:

$$N_{\mathrm{E}} = \frac{4Q_{\mathrm{th}}^2 \varepsilon\varepsilon_0}{e} \left[ \frac{1}{\mu\tau} + \frac{k_{\mathrm{B}}T}{e} \left( \frac{2\pi}{N\Lambda_{\min}} \right)^2 \right], \tag{5}$$

With $Q_{\mathrm{th}} = 3$, $\mu\tau = 10^{-10}\,\mathrm{m^2/V}$ and $\Lambda_{\min} = 4.5\,\mu\mathrm{m}$ for $N = 2$ we get $N_{\mathrm{E}} \approx 4 \times 10^{20}\,\mathrm{m^{-3}}$.

Using the above estimates as an initial fitting parameters the best fit of the experimental data to (3) is performed. The solid lines shown in Fig. 3 are calculated with $\mu\tau = 10^{-10}\,\mathrm{m^2/V}$, $N_{\mathrm{E}} = 4 \times 10^{20}\,\mathrm{m^{-3}}$, and $Q_{\boldsymbol{K}} = 2.7, 3$, and 3.2 for $\boldsymbol{K}/2$, $\boldsymbol{K}/3$, and $\boldsymbol{K}/4$ subharmonic gratings, respectively. Though the set of the fitting parameters may be slightly modified, the perfect qualitative agreement of the experimental data with the theoretical model is evident.

The diffracted beam that occurs in the homogeneously illuminated sample confirms the self-excitation of SCW. It was shown earlier that the photorefractive beam coupling is important for subharmonics generation [13, 16]. It is obviously also important for SCW self-excitation. The incident beam and the self-diffracted beam record a grating with exactly the same grating spacing as the SCW wavelength. This grating reinforces the SCW and vice versa.

There is one practical item that results from direct observation of the beam diffracted from the SCW, which may be used to optimise the spatial frequency of the recording grating for the subharmonics generation. The light-induced grating may become unstable against subharmonics with a grating spacing nearly equal to the wavelength $\Lambda_{\mathrm{SCW}}$ of the SCW self-excited under the same experimental conditions. Otherwise only the beam diffracted from the SCW is observed. If the SCW are strong enough for the detection of the self-diffracted beam the angle $2\theta_{\mathrm{SCW}}$ between transmitted and self-diffracted beam may be easily evaluated. Then, for successful generation of $\boldsymbol{K}/N$ subharmonics, the angle $2\theta$ between the recorded beams should be chosen $N$ times larger than $2\theta_{\mathrm{SCW}} : 2\theta \approx N2\theta_{\mathrm{SCW}}$ ($N\Lambda \approx \Lambda_{\mathrm{SCW}}$).

Finally, let us discuss possible difficulties of subharmonics generation in photorefractive semiconductors. According to the SCW theory the key to subharmonics generation is a high mobility-lifetime product of the free charge carriers [5, 6]. From this point of view the semiconductor crystals may be regarded as well suited for subharmonic generation because they exhibit the largest values of the mobility-lifetime product among all photorefractive materials. Moreover, the theory of SCW was initially developed just for semiconductor crystals [10]. Nevertheless, spatial subharmonics have not been observed in photorefractive semiconductors up to now.

One possible reason analysed theoretically for gallium arsenide [17] is connected to the field-induced reduction of the electron lifetime. Another reason may be the overestimation of the mobility-lifetime product for particular photorefractive semiconductors. In high-resistant photorefractive crystals this value may be much lower than the handbook values typically measured for the relatively low-resistant samples. For example, the product $\mu\tau > 8 \times 10^{-12}\,\mathrm{m^2/V}$ estimated for the photorefractive CdTe sample [18] may still be insufficiently high for subharmonics generation. The next important point is related to the resistivity of the samples. From 50 photorefractive samples available for testing nearly half of them exhibit in the experiments a relatively low resistivity that leads to strong heating by the current through the sample with the voltage applied, or even do not permit an electric field higher than 1 kV/cm to be applied.

Therefore, for the successful generation of spatial subharmonics the semiconductor must combine high resistivity, good photorefractive properties and a high mobility-lifetime product. The experiments performed in the course of the present work show that only a relatively small part of the photorefractive CdTe:Ge samples meet all these requirements.

## 3 Conclusions

The described experiments with CdTe:Ge prove the possibility of observing spatial subharmonics in crystals other than sillenites, particularly in photorefractive semiconductors. The amplitude of the external square-shaped electric field controls which one of the secondary gratings is generated in the studied CdTe sample. The range of the grating vectors of the primary grating is defined where subharmonics occur and the threshold ac amplitudes are measured for different subharmonic gratings at different spatial frequencies of the principal grating. The data of the threshold dependencies enable an evaluation of the mobility-lifetime product and the effective trap density for the studied sample using the SCW theoretical model of subharmonics generation. Self-excitation of SCW is observed in a homogeneously illuminated ac-biased CdTe sample. The sharp, well developed light beam is generated because of diffraction of the incident beam from this SCW and further photorefractive self-amplification. It is shown that SCW self-excitation affects photorefractive subharmonics generation.

*Acknowledgements.* The author is grateful to S. Odoulov for valuable remarks, D.J. Webb, L. Solymar, and M. Vasnetsov for their expert introduction to the subharmonics experiments, K.H. Ringhofer and B. Sturman for stimulating discussions. CdTe samples were grown by Z. Zakharuk and I. Rarenko. Financial support of INTAS (grant YSF 99-4048 ) is gratefully acknowledged.

## References

1. S. Mallick, B. Imbert, H. Ducollet, J.-P. Herriau, J.-P. Huignard: J. Appl. Phys. **63**, 5660 (1988)
2. J. Takacs, M. Schaub, L. Solymar: Opt. Commun. **91**, 252 (1992)
3. J. Richter, A. Grunnet-Jepsen, J. Takacs, L. Solymar: IEEE J. Quantum Electron. **QE-30**, 1645 (1994)
4. J. Takacs, L. Solymar: Opt. Lett. **17**, 247 (1992)
5. B. Sturman, A. Bledowski, J. Otten, K. Ringhofer: J. Opt. Soc. Am B **9**, 672 (1992)
6. B. Sturman, A. Bledowski, J. Otten, K. Ringhofer: J. Opt. Soc. Am B **10**, 1919 (1993)
7. O.P. Nestiorkin: Opt. Commun. **81**, 315 (1991)
8. V.V. Shepelevich, E.M. Khramovich: Sov. Opt. Spectrosc. **65**, 240 (1988)
9. S.G. Odoulov, S.S. Slussarenko, K.V. Shcherbin: Sov. Tech. Phys. Lett. **15**, 417 (1989)
10. R.F. Kazarinov, R.A. Suris, B.I. Fuks: Sov. Phys. Semicond. **7**, 480 (1973)
11. H. Rajbenbach, A. Delboulbé, J.P. Huignard: Opt. Lett. **14**, 1275 (1989)
12. S. Lyuksyutov, P. Buchhave, M. Vasnetsov: Phys. Rev. Lett. **79**, 67 (1997)
13. H.C. Pedersen, P.M. Johansen, D.J. Webb: J. Opt. Soc. Am. B **15**, 1528 (1998)
14. A. Novikov, S. Odoulov, R. Jungen, T. Tschudi: J. Opt. Soc. Am. B **9**, 1654 (1992)
15. M.P. Petrov, V.V. Bryksin, V.M. Petrov, S. Wevering, E. Krätzig: Phys. Rev. A **60**, 2413 (1999)
16. H.C. Pedersen, D.J. Webb, P.M. Johansen: J. Opt. Soc. Am. B **15**, 2439 (1998)
17. B.I. Sturman, M. Aguilar, F. Agulló-López: Phys. Rev. B **54**, 13737 (1996)
18. K. Shcherbin, A. Shumeljuk, S. Odoulov, P. Fochuk, G. Brost: SPIE Proc. **2795**, 236 (1996)